Low Profile Ultrathin Wide-Passband Polarization-insensitive Frequency Selective Surface with wide angular stability

Garima Tiwari[1], Manshree Mishra[1], Pramod Kumar Gupta[1], Trivesh Kumar[1], Biswajeet Mukherjee[2]

[1]Department of Electronics & Communication, PDPM Indian Institute of Information Technology Design and Manufacturing, Jabalpur, India
[2]Department of Electronics Science, Delhi University, Delhi, India

Corresponding author: Garima Tiwari (e-mail: garima.tiwari29@gmail.com).

ABSTRACT In this paper, a low profile, ultrathin, wide passband, polarization insensitive, wide angular stable frequency selective surface (FSS) is proposed. The structure is realized on a two-sided copper on Roger's RT 5880 substrate with 0.51 mm thickness. The top layer design consists of a combination of slotted circle with quad arcs along with cross bars at the center with diagonal tilts at the corner. On the bottom layer, an elliptical-shaped patch is placed at the center. This elliptical patch at the bottom layer of FSS helps to realize the wide pass-band response. The pass-band bandwidth ranges from 8.45 to 9.45 GHz centered at 8.96 GHz. The proposed FSS is polarization insensitive. The structure provides angular stability till 45° of incident angle for Transverse Electric (TE) and Transverse Magnetic (TM) modes of operation. The prototype of FSS is fabricated with an array of 10 x 10-unit cells. The simulated and measured results are found to be in good agreement.

INDEX TERMS Frequency Selective surface, polarization insensitive, ultrathin, wide passband.

I. INTRODUCTION

FREQUENCY selective surface (FSS) is an array structure of periodic metallic patches, slots or apertures with the capability to associate with incident electromagnetic (EM) wave [1]. It has the capability of transmitting or reflecting the incident EM wave for specific frequency range [2]. It finds application in spatial filters, band stop filters [3], absorbers, radomes [4] antenna reflectors [5], Electromagnetic shielding [6], artificial magnetic conductors [7] and polarization convertors [8]. The change in the incident angle and polarization of the incident EM wave changes the resonant frequency, reflection, and transmission responses of FSS. To achieve a response insensitive to polarization and incident angle remains challenging. To achieve wideband response in FSS, researchers have reported various design aspects like; multilayer structures [9], FSS with active components like varactor diodes [10], multi-dimensional structures like 2.5 D hexagonal arrangement [11], composite structures or textile structures [12] etc. All these structures are high profile, complicated, and expensive to fabricate. A wideband response using a low-profile structure is desirable.

In this work, a low profile, wide passband, ultrathin, polarization insensitive Frequency selective surface is investigated. The proposed FSS has a metallic structure on the top layer and the bottom layer of Roger's 5880 substrate. Through this low-profile structure with a unit cell of physical size 9.6 mm x 9.6 mm ($0.42\lambda_g$ x $0.42\ \lambda_g$), a wide band response from 8.45 to 9.45 GHz centered at 8.96 GHz is achieved. The FSS characteristics are examined by reflection and transmission characteristics at different incident angles and polarization angles. An equivalent circuit model is also developed and validated with the full wave simulated result, which is experimentally verified using a fabricated prototype.

II. DESIGN METHODOLOGY

A. UNIT CELL GEOMETRICAL CONFIGURATION

The Geometrical configuration of the proposed structure consists of the top metallic layer, middle layer substrate of Roger's RT 5880 having a dielectric constant of 2.2, the loss tangent of 0.0009, the thickness of 0.51 mm, and bottom layer of copper along with the perspective view, as shown in fig.1-(a). The metal thickness is 0.035 mm for both top and bottom layer. The top layer consists of combination of self-patterned geometries of cross dipole and quad-circular arcs with slots inside it. The structure on the bottom layer consists of elliptical patch. The optimized dimensions are a_1=9.6 mm, a_2=0.4 mm, a_3=0.2 mm, a_4=0.2 mm, a_5=2.67 mm, a_6=6.65 mm, a_7=4.7 mm, a_8=6.4 mm, a_9=4.8mm. The proposed FSS unit cell is simulated using CST microwave studio available

commercially. The simulated results depicting reflectivity and transmittivity characteristics are as shown in fig.1-(b). It is evident that the designed FSS shows a band pass response at a resonant frequency of 8.96 GHz with a bandwidth of 1 GHz from 8.45 GHz to 9.45 GHz, as depicted by the highlighted portion. At a resonant frequency of 8.96 GHz, the periodicity of unit cell is 0.42λg and the thickness of FSS is 0.022λg, where λg is the guided wavelength.

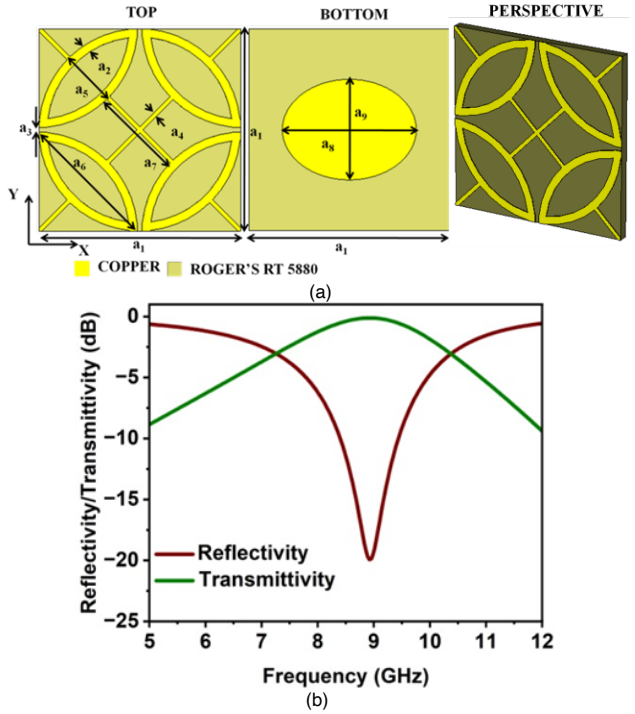

FIGURE 1. Proposed Frequency selective surface unit cell with (a) top, bottom and perspective layer structure, (b) Reflectivity and Transmittivity of proposed Frequency selective surface

B. Design steps

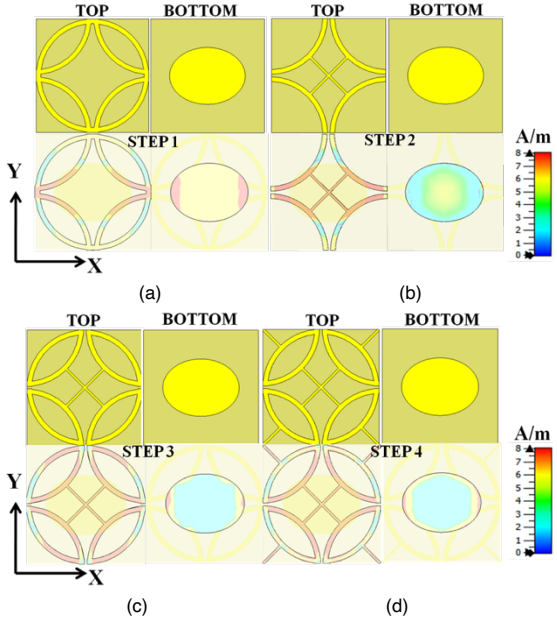

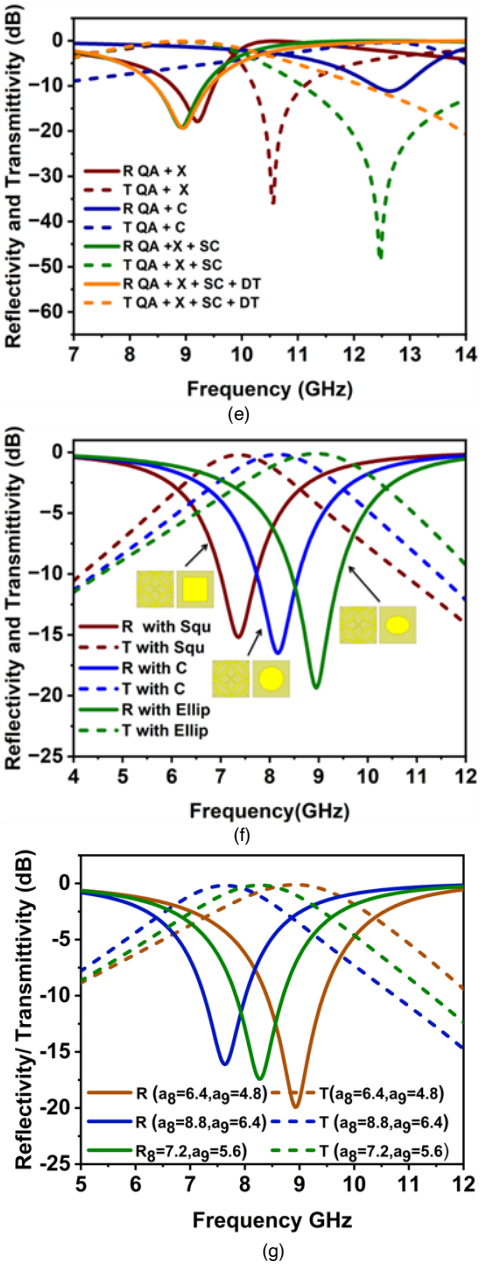

FIGURE 2. Design Methodology structure with corresponding surface current distribution (a). Step 1-circular ring with quad circular arcs at the top layer and elliptical patch at the bottom layer, (b). Step 2- Quad circular arcs with cross bar at the top layer and elliptical patch at the bottom layer, (c). Step 3- Quad circular arcs and slotted circular ring with cross bar at the top layer and elliptical patch at the bottom layer, (d). Step 4- Quad circular arcs and slotted circular ring with cross bar and tilted bar on edges at the top layer and elliptical patch at the bottom layer (e). Simulated reflectivity and transmittivity for each step 1-4, (f). Simulated reflectivity and transmittivity for - Quad circular arcs and slotted circular ring with cross bar and tilted bar on edges at the top layer and square, circular and elliptical patches at the bottom layer, (g). Simulated reflectivity and transmittivity for effect of variation in size of elliptical patch at the bottom layer.

The design steps of top and bottom surface along with the current distribution at the top and bottom surface are explained in fig. 2-(a)-(d) with comparative simulated reflectivity curve as shown in Fig. 2-(e). The design initially begins with a circular ring (C) with quad circular arcs (QA) on the top and

elliptical patch at the bottom as shown in fig.2-(a) as shown in step 1.

A single frequency band response at 9.24 GHz is achieved as shown in fig. 2-(e). However, the passband of this FSS structure is of 0.72 GHz. From the surface current distribution, it is observed that the current is dominant at the edges of quad circular arcs on the top and at the edges of elliptical patch on the bottom.

In step 2, cross bar (X) structure is introduced along the quarter circular arcs on the top layer with same elliptical patch at the bottom layer, as shown in Fig. 2-(b). This structure offers a passband of 0.8 GHz at frequency centered at 9.21 GHz as shown in Fig. 2-(e). The surface current is dominant at the quad circular arcs and the cross-bar structure at the center on the top surface where as for the bottom layer the surface current is dominant at the center.

In step 3, slotted circular ring (SC) along with the quad circular arcs and the cross-bar structure on the top layer with the same elliptical patch structure at the bottom, is proposed as depicted in Fig. 2-(c). Now the passband bandwidth is increases to 0.9 GHz centered at 8.8 GHz. Due to introduction of slotted circular ring along with the quad circular arcs and the cross-bar structure, the surface current is dominants at the center and distributes towards the edges on the top layer and on the bottom layer surface current is dominant at the edges.

In step 4 diagonal tilted bars (DT) at the edges of unit cell along with the structure of step 3 is introduced as shown in Fig. 2-(d), due to which the surface current is dominant at the center distributing towards the edges and for the bottom layer current is dominant at the edges which results in a wider passband width of 1 GHz centered at 8.96GHz.

Further Top layer structure is analyzed with the changes in bottom layer with square, circular and elliptical patch structure. Top layer structure comprises of Slotted circular ring, quad circular arc, cross bar structure and tilted diagonal bars. With square patch of size length 6.4 mm a bandwidth of 0.5 GHz centered at 12.64 GHz is obtained. With circular patch of radius 6.4 mm a pass bandwidth of 0.7 GHz is obtained; whereas with elliptical patch with major axis length of 6.4 mm and minor axis length of 4.8 mm, a pass band width of 1 GHz is obtained as depicted in Fig. 2-(f) As larger bandwidth is obtained from elliptical path therefore in the final design elliptical patch is considered at the bottom layer. This elliptical patch at the bottom layer, size is varied for various values of a_8 and a_9 as shown in Fig. 2-(g), the maximum bandwidth is obtained for the case of optimized dimension of a_8=6.4 and a_9=4.8 mm.

C. Study of Polarization insensitivity and incidence angle variation

To better understand the physical insight of the mechanism of the proposed FSS structure the electric field and surface current plots are analyzed at the resonant frequency of 8.96 GHz. Fig. 3-(a) and 3-(b) represent the scalar electric field distribution plot for TE and TM mode respectively for both top and bottom layer structures. On the top layer the electric field is dominant along the split circular arcs at the edges of the unit cell and decreases towards the center. And for the bottom layer electric field is dominant at the edges of the elliptical patch. The strong electric field evidences the existence of strong electrical resonance, which is due to coupling of metallic upper and lower layer and the dielectric substrate. The concentration of electric field in upper and lower layer is responsible for electric excitation. These simultaneous Electric and magnetic excitations realizes maximum reflection coefficient at the resonant frequency of 8.96 GHz. The surface current distribution plot for top and bottom layer structures at 8.96 GHz is shown in fig. 3-(c) and 3-(d) respectively.

The surface current on the upper layer is dominant at the center of the unit cell along the cross-dipole structure and distributes towards the edges of the circular arcs, whereas on the lower layer the surface current is dominant at the center of the elliptical patch. It is observed that the surface current distribution in the upper and lower layers is anti-parallel and constitute circular loop driven by incident magnetic field. This circulating current is responsible for magnetic excitation.

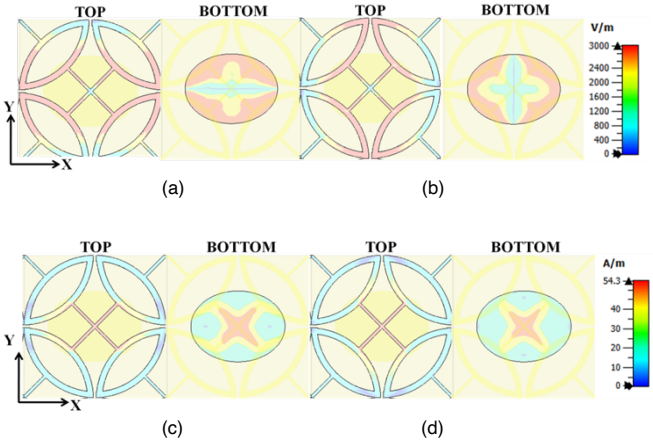

FIGURE. 3. Simulated curves for proposed FSS (a). Scalar Electric field distribution for TE mode, (b). Scalar Electric field distribution for TM mode, (c). Surface current distribution for TE mode, (d).Surface current distribution for TM mode

The polarization stability for the proposed FSS is depicted in Fig. 4-(a) which exhibits simulated reflectivity and transmittivity curves for the EM wave incident normally with different polarization angles. The Electric and magnetic fields are rotated at different polarization angles varying between 0° to 90° with step size of 15° values, while the direction of EM propagating waves remains fixed. For different polarization angles, the proposed symmetric structure at center, the polarization angle is varied from between 0° to 90°.

Further the designed FSS, the reflectivity and transmittivity for the Transverse Electric (TE) and Transverse Magnetic (TM) polarization are depicted in Fig. 4-(b) and 4-(c) respectively. For TE polarization, the direction of electric field is fixed while the direction of EM wave propagation and magnetic field rotates for various incidence angles. For the case of TM polarization, the direction of magnetic field is fixed while the direction of EM wave propagation and electric field rotates for various incidence angles. For the designed FSS it is observed that for both TE and TM polarization, the

structure offers similar reflectivity up to 45°of incidence angle. Thus the FSS offers angular stability till 45°.

III. EQUIVALENT CIRCUIT MODEL

The equivalent circuit model for the proposed absorber is shown in Fig.5-(a). The Top layer structure is represented by a series L-C circuit and is connected in parallel with the equivalent L-C circuit of the bottom layer structure. For the top layer structure surface current is dominant along the cross-bar structure at the center and the corners of the unit cell. Due

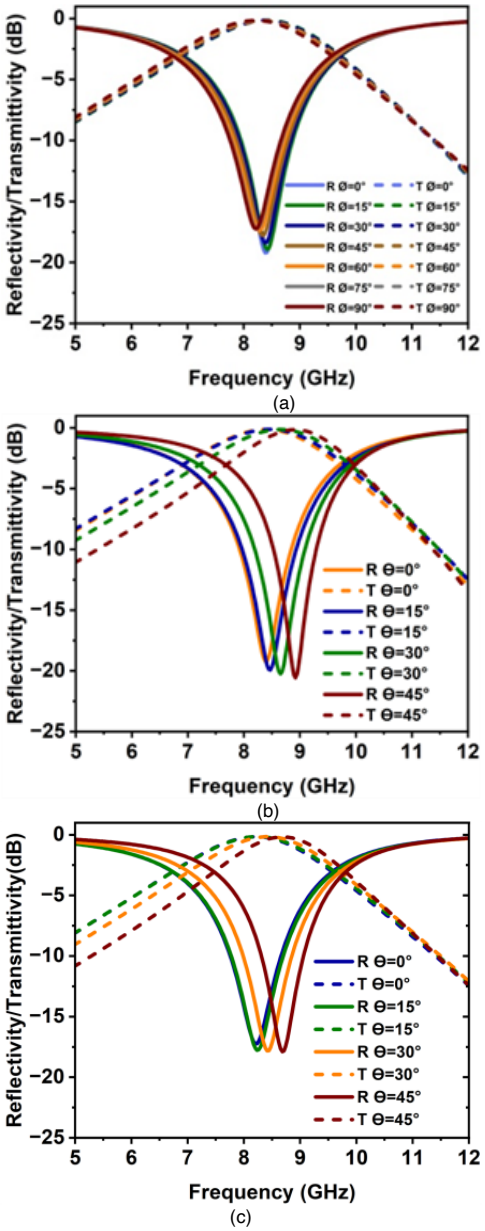

FIGURE. 4. Simulated Reflectivity and Transmittivity curves of Proposed Frequency selective surface at different (a). Polarization angles, (b). Incidence angles for TE polarization, (c). Incidence angles for TM polarization

to presence of a strong surface current distribution, inductive effect is dominant. This inductive effect is modeled as L_1 and L_3 in the circuit model. Moreover, Electric field is dominant at edges of quarter circular arcs near the slot. Due to accumulation of charges, capacitive loading effect is dominant at the edges near slot, along with the inductive loading at the middle of the quarter circular arcs. This is represented by LC tank circuit with L_2 and C_1 in the circuit model. For the bottom layer of the structure, surface current is dominant at the center causing inductive effect represented by L_4 in the circuit model. Also, the electric field is dominant towards the edges of the elliptical patch which introduces capacitive effect represented by C_2 and C_3 in the circuit model. The calculated lumped parameters for the equivalent circuit of the proposed absorber are L_1=1000 nH, C_1=500 fF, L_2=1nH, C_2=21 fF, L_3=100 nH, C_3=25 fF, L_4=27.5 nH. The lumped elements response for the equivalent circuit and the CST reflectivity curve of the EM model resonant frequency of 8.96 GHz as shown in Fig. 5-(b), are in a good agreement with each other.

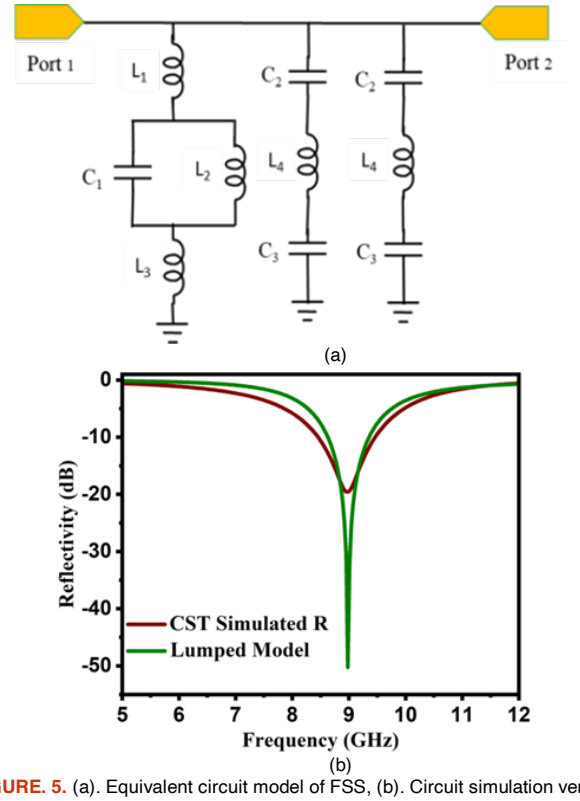

FIGURE. 5. (a). Equivalent circuit model of FSS, (b). Circuit simulation versus CST simulated reflectivity curve

IV. EXPERIMENTAL RESULTS & DISCUSSION

Fig. 6-(a) and 6-(b) depicts the fabricated prototype top and bottom layer of the proposed FSS, with insight image showing the zoomed image of the fabricated structure. An array of 10 x 10 unit cells with structure on the top layer and the bottom layer are fabricated on 0.51mm thick Roger RT 5880 substrate. The structure is fabricated using ENTHU technology ETS PCBMATE-300W PCB prototype milling based machine. The measurement setup for proposed FSS consists of two broadband horn antennas, fabricated prototype structure, holder for holding the prototype and vector network analyzer. The reflection coefficient for the fabricated FSS is

measured using Agilent E5071C series vector network analyzer in the anechoic chamber.

Fig.6-(c). depicts the simulated and measured reflection coefficient for the fabricated FSS which are in close agreement to each other. The measured reflectivity ranges from 8.47 GHz to 9.45 GHz whereas the simulated reflectivity is from 8.45 GHz to 9.45 GHz. Slight differences in the simulated and measured results may arise due to fabrication tolerances, cable losses, etc.

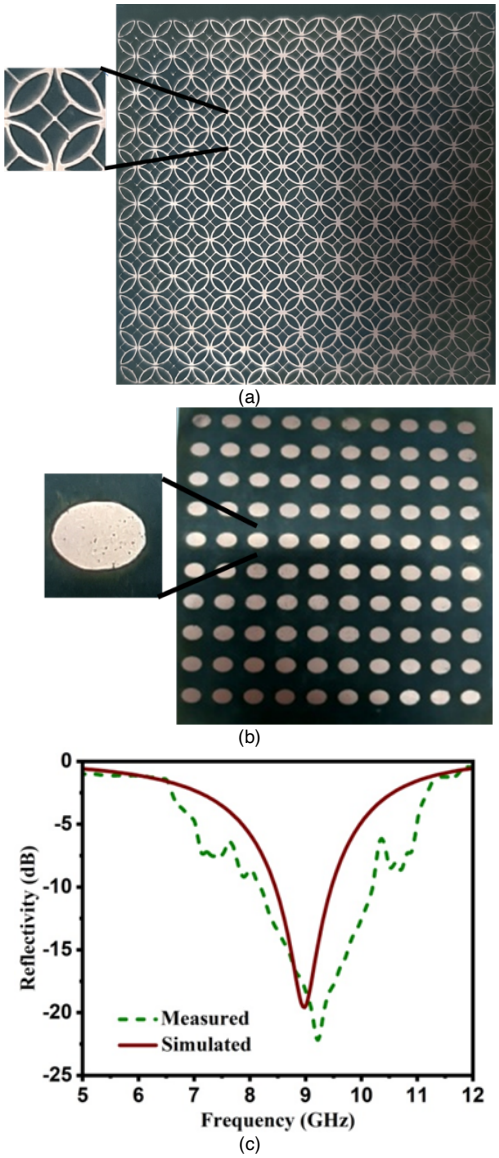

FIGURE. 6. Prototype developed of the proposed FSS (a).Top Layer, (b).bottom layer, (c).Simulated and measured Reflectivity curve for the proposed FSS

Table I shows the comparison of the proposed structure with the state of art. The proposed FSS has a unique pattern design, which is very compact in size and thickness of 0.51mm only. With the introduction of elliptical patch in the bottom layer, a bandwidth of 1 GHz from 8.45 to 9.45 GHz centered at 8.96 GHz is achieved. Also, the structure is polarization insensitive providing angular stability till 45°.

TABLE I. Comparison Table

Ref	Size X λg x Y λg x Z λg	BW (GHz)	OF	AS	DC	PI
[13]	0.52 x 0.52 x 0.201	13.7 to 15.6 (1.9)	9.3	NM	4.4	NM
[14]	0.23 x 0.23 x 0.029	5.94	5.94	85°	2.2	NM
[15]	0.08 x 0.08 x 0.005	0.85 to 1.1 (0.25)	1.14	60°	4.4	YES
[16]	0.47 x 0.47 x 0.008	200 MHz	6.4	NM	2.2	YES
[17]	0.52 x 0.52 x 0.31	1.13 to 2.09 (0.96)	2.42	45°	4.7	NM
[18]	0.11 x 0.11 x 0.17	3.2 to 3.4 (0.2)	3.3	60°	2.2	NM
[PW]	**0.42 x 0.42 x 0.022**	**8.45 to 9.45 (1)**	**8.96**	**45°**	**2.2**	**YES**

REF = Reference, BW = Bandwidth, OF = Operating Frequency, AS = Angular stability, DC = Dielectric constant, PI = Polarization Insensitive, PW = Present work, NM = Not mentioned.

V. CONCLUSION

This paper presents an ultra thin, wide passband, polarization independent Frequency selective structure. The proposed Frequency selective surface is compact with dimensions 0.42λg x 0.42λg x 0.022λg. Due to introduction of elliptical patch in the FSS design, the proposed structure provides a wide bandwidth of 1 GHz from 8.45 GHZ to 9.45 GHz centered at 8.96 GHz. The FSS is polarization insensitive and provides wide angular stability till 45°. This proposed FSS structure can be used for microwave and defense applications.

REFERENCES

[1] B. A. Munk, “Frequency Selective Surfaces: Theory and Design,” Wiley, New York, 2000

[2] T. K. Wu, “Frequency Selective Surface and Grid Array”. New York, NY, USA: Wiley, 1995

[3] S. Das, A. Rajput and B. Mukherjee, "A Novel FSS-Based Bandstop Filter for TE/TM Polarization," in IEEE *Letters on Electromagnetic Compatibility Practice and Applications*, vol. 6, no. 1, pp. 11-15, March 2024, doi: 10.1109/LEMCPA.2023.3327027.

[4] Y. Ranga, L. Matekovits, K. P. Esselle and A. R. Weily, "Multioctave Frequency Selective Surface Reflector for Ultrawideband Antennas," in IEEE Antennas and Wireless Propagation Letters, vol. 10, pp. 219-222, 2011, doi: 10.1109/LAWP.2011.2130509.

[5] Y.-M. Yu, C.-N. Chiu, Y.-P. Chiou, and T.-L. Wu, “An effective via-based frequency adjustment and minimization methodology for single-layered frequency-selective surfaces,” IEEE Trans. Antennas Propag., vol. 63, no. 4, pp. 1641–1649, Apr. 2015

[6] S. Ghosh and K. V. Srivastava, “Broadband polarization-insensitive tunable frequency selective surface for wideband shielding,” IEEE Trans. Electromagn. Compat., vol. 60, no. 1, pp. 166–172, Feb. 2018.

[7] S. M. Rouzegar, A. Alighanbari, and O. M. Ramahi, “Wideband uniplanar artificial magnetic conductors based on curved coupled

microstrip line resonators," IEEE Microw. Wireless Compon. Lett., vol. 27, no. 4, pp. 326–328, Apr. 2017
[8] H. Chen et al., "Ultra-wideband polarization conversion metasurfaces based on multiple plasmon resonances," J. Appl. Phys., vol. 115, 2014, Art. no. 154504.
[9] Q. Luo, S. Gao, M. Sobhy, and X. Yang, "Wideband transmitarray with reduced profile," IEEE Antennas Wireless Propag. Lett., vol. 17, no. 3, pp. 450–453, Mar. 2018.
[10] R. Sivasamy, B. Moorthy, M. Kanagasabai, V. R. Samsingh, and M. G. N. Alsath, "A wideband frequency tunable FSS for electromagnetic shielding applications," IEEE Trans. Electromagn. Compat., vol. 60, no. 1, pp. 280– 283, Feb. 2018.
[11] S. Ghosh and K. V. Srivastava, "A polarization-independent broadband multilayer switchable absorber using active frequency selective surface," IEEE Antennas Wireless Propag. Lett., vol. 16, pp. 3147–3150, 2017
[12] L. Alonso-González, S. Ver-Hoeye, M. Fernández-García and F. Las-Heras Andrés, "Broadband Flexible Fully Textile-Integrated Bandstop Frequency Selective Surface," in IEEE Transactions on Antennas and Propagation, vol. 66, no. 10, pp. 5291-5299, Oct. 2018, doi: 10.1109/TAP.2018.2858141.
[13] S. Chakravarty and D. Mitra, "A Novel Ultra-Wideband and Multifunctional Reflective Polarization Converter," 2020 IEEE 17th India Council International Conference (INDICON), New Delhi, India, 2020, pp. 1-4, doi: 10.1109/INDICON49873.2020.9342188.
[14] T. Hong, W. Xing, Q. Zhao, Y. Gu and S. Gong, "Single-Layer Frequency Selective Surface With Angular Stability Property," in IEEE Antennas and Wireless Propagation Letters, vol. 17, no. 4, pp. 547-550, April 2018, doi: 10.1109/LAWP.2018.2801864.
[15] T. Cheng, Z. Jia, T. Hong, W. Jiang and S. Gong, "Dual-Band Frequency Selective Surface With Compact Dimension and Low Frequency Ratio," in IEEE Access, vol. 8, pp. 185399-185404, 2020, doi: 10.1109/ACCESS.2020.3030131.
[16] M. M. Zargar, A. Rajput, K. Saurav and S. K. Koul, "Single-Layered Flexible Dual TransmissiveRasorbersWith Dual/Triple Absorption Bands for Conformal Applications," in IEEE Access, vol. 9, pp. 150426-150442, 2021, doi: 10.1109/ACCESS.2021.3126197.
[17] Y. Li, P. Ren, Z. Xiang and B. Xu, "Design of Miniaturized Frequency-Selective RasorberWith Embedded Dual-Bow Resonators," in IEEE Antennas and Wireless Propagation Letters, vol. 22, no. 2, pp. 442-446, Feb. 2023, doi: 10.1109/LAWP.2022.3216039.
[18] W. Afzal, A. Ebrahimi, M. R. Robel and W. S. T. Rowe, "Low-Profile Higher-Order Narrowband Bandpass Miniaturized-Element Frequency-Selective Surface," in IEEE Transactions on Antennas and Propagation, vol. 71, no. 4, pp. 3736-3740, April 2023, doi: 10.1109/TAP.2023.3239171.